Int J Appl Earth Obs Geoinformation 90 (2020) 102070

Contents lists available at ScienceDirect

Int J Appl Earth Obs Geoinformation

journal homepage: www.elsevier.com/locate/jag

Moving from plot-based to hillslope-scale assessments of savanna vegetation structure with long-range terrestrial laser scanning (LR-TLS)

Jenia Singh[a,*], Shaun R. Levick[a,b], Marcus Guderle[a], Christiane Schmullius[c]

[a] Max Planck Institute for Biogeochemistry, Hans-Knoell-Str. 10, 07745 Jena, Germany
[b] CSIRO Land and Water, PMB 44, Winnellie, NT 0822, Australia
[c] Department of Earth Observation, Friedrich-Schiller-University Jena, Grietgasse 6, 07743 Jena, Germany

ARTICLE INFO

Keywords:
LiDAR
Long-range scanning
Savanna structure
Canopy height
Canopy cover
Vertical profiles

ABSTRACT

Reliable quantification of savanna vegetation structure is critical for accurate carbon accounting and biodiversity assessment under changing climate and land-use conditions. Inventories of fine-scale vegetation structural attributes are typically conducted from field-based plots or transects, while large-area monitoring relies on a combination of airborne and satellite remote sensing. Both of these approaches have their strengths and limitations, but terrestrial laser scanning (TLS) has emerged as the benchmark for vegetation structural parameterization – recording and quantifying 3D structural detail that is not possible from manual field-based or airborne/spaceborne methods. However, traditional TLS approaches suffer from similar spatial constraints as field-based inventories. Given their small areal coverage, standard TLS plots may fail to capture the heterogeneity of landscapes in which they are embedded. Here we test the potential of long-range (> 2000 m) terrestrial laser scanning (LR-TLS) to provide rapid and robust assessment of savanna vegetation 3D structure at hillslope scales. We used LR-TLS to sample entire savanna hillslopes from topographic vantage points and collected coincident plot-scale (1 ha) TLS scans at increasing distances from the LR-TLS station. We merged multiple TLS scans at the plot scale to provide the reference structure, and evaluated how 3D metrics derived from LR-TLS deviated from this baseline with increasing distance. Our results show that despite diluted point density and increased beam divergence with distance, LR-TLS can reliably characterize tree height (RMSE = 0.25–1.45 m) and canopy cover (RMSE = 5.67–15.91%) at distances of up to 500 m in open savanna woodlands. When aggregated to the same sampling grain as leading spaceborne vegetation products (10–30 m), our findings show potential for LR-TLS to play a key role in constraining satellite-based structural estimates in savannas over larger areas than traditional TLS sampling can provide.

1. Introduction

Savannas are heterogeneous ecosystems composed of mixed-tree grass communities that cover 20% of the global vegetated land surface (Scholes and Archer, 1997). Given their significant contribution to terrestrial net primary production (1–12 Mg ha^{-1} yr^{-1}), savannas are important for the regulation of the global carbon cycle (Grace et al., 2006). However, understanding of savanna structural dynamics and their carbon sequestration potential remains limited in the face of global environmental (Williams et al., 2004; Wigley et al., 2010; Buitenwerf et al., 2012; Stevens et al., 2017) and land-use changes (Archibald et al., 2013). To effectively implement sustainable land management practices, while at the same time maintaining a range of tree-grass mixtures for biodiversity conservation, savanna ecosystems warrant comprehensive and timely inventory efforts. Structural information is not only fundamental to advancing savanna ecological process understanding, but also assists in the development of baseline information required for global carbon emission agreements (e.g. REDD +). Therefore, regular monitoring campaigns are necessary to characterize and map savanna vegetation structure under diverse land-use conditions.

Mapping savanna vegetation structure is challenging due to heterogeneity at hillslope and regional scales that arises from the interaction of topography, soils, climate and biological factors (Meyer et al., 2007; Levick and Rogers, 2011; Sankaran et al., 2008; Vaughn et al., 2015). Most of our current understanding of savanna vegetation structure derives from field-based measurements using either plots or transects. While such field data can be scaled to larger extents with remote sensing imagery (Lucas and Armston, 2007; Boggs, 2010), their limited spatial coverage means they may fail to account for variable

* Corresponding author.
E-mail address: jsingh@bgc-jena.mpg.de (J. Singh).

https://doi.org/10.1016/j.jag.2020.102070
Received 9 September 2019; Received in revised form 3 February 2020; Accepted 4 February 2020
Available online 02 April 2020

vegetation structure across the landscape (Asner et al., 2009; Mathieu et al., 2013). In response, there has been growing interest in the use of light detection and ranging (LiDAR) to augment traditional field measurements (Dubayah and Drake, 2000; Lefsky et al., 2002; Asner et al., 2007) with high-resolution 3D data of vegetation canopies. LiDAR data can be acquired from spaceborne, airborne or terrestrial sensors, with each sensor meeting different vegetation mapping needs (Urbazaev et al., 2015; Levick and Rogers, 2008; Staben et al., 2018), improving predictions and minimizing extrapolation errors (Frazer et al., 2011). A key advantage of airborne LiDAR is wide geographic coverage but detection of smaller trees and shrubs, which are important components of savanna ecosystem functioning, is still challenging.

The last decade has witnessed a growing interest in ground-based LiDAR, or terrestrial laser scanning (TLS), for high precision 3D quantification of vegetation structure. TLS instruments facilitate unprecedented spatial structure and reflective representation of vegetation components, right down to individual branch and leaf scales (Dassot et al., 2012; Newnham et al., 2015). 3D data collected from TLS is considered to capture a much more holistic representation of vegetation structure than can possibly be achieved through manual fieldwork, and has successfully been applied as an effective and accurate approach to calibrate vegetation models (Dittmann et al., 2017; Calders et al., 2018), and define stand structural diversity (Ehbrecht et al., 2017). Also, metaproperties from TLS such as laser returns, intensity and distance can reflect the underlying conditions of the ecosystem (Paynter et al., 2018). Key geometrical attributes including tree height (Hopkinson et al., 2004; Strahler et al., 2008), vertical height profiles (Singh et al., 2018) and canopy structure (Hardiman et al., 2018) can be reconstructed and measured with high accuracy from TLS data. Besides basic vegetation attributes, TLS point clouds enable non-destructive approaches to quantify canopy and stem volume, which reduces uncertainties in biomass estimations that arise from conventional inventory methods (Calders et al., 2015; Disney et al., 2018; Stovall et al., 2018; Gonzalez de Tanago et al., 2018).

Realization of the ecological importance of the 3D information that TLS provides has led to optimizations in data acquisition and processing. The acquisition of single scan TLS measurements offers a rapid and efficient means of characterizing vegetation structure (Liang et al., 2016), due to reduced field effort and faster post-processing, thereby enabling data acquisition at a greater number of sampling points. Single scan approaches have been successfully used for the estimation of canopy cover (Muir et al., 2018), wood volume (Astrup et al., 2014), basal area measurement (Seidel and Ammer, 2014) and vertical plant profiles (Calders et al., 2014). However single scan approaches can physically only sample one side of a tree and are more prone to occlusion of distant vegetation by the foreground elements (Strahler et al., 2008; Hilker et al., 2010; Wilkes et al., 2017). The degree of occlusion within a single scan is influenced directly by the vegetation structure, tree stand density and plot size (Olofsson and Olsson, 2018). A systematic multiple scanning approach with subsequent co-registration of scans reduces this occlusion effect (Wilkes et al., 2017), and has been shown to produce improved accuracy of vegetation structural metrics (Calders et al., 2015; Saarinen et al., 2017). The additional setup time and logistics associated with multiple position scanning (Wilkes et al., 2017) can lead to similar to that required for manual field inventories of vegetation structure (Newnham et al., 2015), and this often constrains the TLS measurements to plot-scales (< 1 ha).

Much of the progress to date in TLS measurement of vegetation structure has taken place in temperate and tropical forested systems. As such, the sampling range of common TLS sensors has not been considered a limiting factor, since field of view seldom exceeds sensor range. In open systems like savannas, field of view can greatly exceed the sampling range of common TLS sensors. However recent breakthroughs in time-of-flight LiDAR sensor technology have dramatically increased the usable sampling range of TLS sensors, with some providers now offering ranges of up to 6000 m (e.g. Riegl VZ-6000). These instruments have the potential to map entire hillslopes from a suitable vantage point with a single scan approach, allowing capture of data at 10–100's ha scales. Long-range terrestrial laser scanning (LR-TLS) necessitates trade-offs between laser energy and pulse frequency, where increasing pulse energy subsequently reduces the laser pulse frequency and increases scanning time. Although laser beams are coherent light energy, most sensors are subject to a degree of beam divergence, meaning that the width of the beam (footprint) increases with distance from the scanner. Over the short distances typical of plot-based TLS approaches this is of little consequence, but understanding the effects of beam diverge on the retrieval of the vegetation structure parameter becomes important when considering long-range scanning.

In this study, we aimed to assess the potential of LR-TLS scans for extracting key structural attributes of savanna woody vegetation at hillslope scales. Specifically, we explore how structural measurements from LR-TLS degrade with distance from the scanner, and identify the distances over which LR-TLS can be reliably used for 3D structural characterization.

2. Methods

2.1. Study area

This study was conducted in the semi-arid savanna landscapes of Kruger National Park (KNP), South Africa (23°98′S, 31°55′E) (Fig. 1). KNP is a national reserve located in north-eastern South Africa that encompasses an area of almost 2 million ha. We focused on two sites in the south-western part of the park, using natural vantage points at Mathekinyani and Stevenson Hamilton lookouts (Fig. 1). The areas around these vantage points comprise of flat and low slope terrain that are dominated by the short height class and broad canopies of semi-deciduous *Combretums* and *Accacia nigrescens*, which occur in a matrix of evergreen *Euclea divinorum* (Gertenbach, 1983). Woody canopy cover ranges from as low as 20% to near closed canopy cover of 50% across dispersed trees and shrubs, and closed woodlands of more than 80% cover in riparian areas (Table 1). The region has a mean annual rainfall of 550 mm yr^{-1}, most of which falls between October and March (MacFadyen et al., 2018). Soils in most of the south-western KNP are derived from granite substrates which are nutrient-poor, and exhibit significant catenal variations from deep sand and loam on upland to duplex sodic soil on bottomlands (Venter, 1986).

2.2. Terrestrial LiDAR sampling at landscape and plot-scales

Both sites were mapped in October 2016 (late dry season) using a Riegl VZ-2000 terrestrial laser scanning system (RIEGL Laser Measurement Systems GmbH). The RIEGL VZ-2000 is a multiple return long-range 3D scanner, which operates in the near-infrared spectrum (1550 nm) and produces a beam divergence of 0.35 mrad. The instrument provides the 3D information at a rate of 400,000 measurements s^{-1}, and the measurements can be obtained up to a distance of 2500 m on a natural surface. The inclination sensor provides rotation matrices (roll, yaw and pitch) of the scanner, allowing for accurate projection of the laser pulses. To improve the accuracy of the 3D positioning, LiDAR laser ranges were combined with an external differential Leica GS14 GNSS GPS (accuracy < 3 cm).

The landscape scanning design consisted of acquiring single long-range scans from elevated vantage points. Scans were taken with an azimuth and zenith range of 180° and 100° respectively. The scanner settings were the same at both sites and are summarized in Table 2. This scanning setup resulted in a mean point density of 158.6 laser returns per m^2 at 100 m to 6.02 laser returns per m^2 at a distance of 600 m.

In each landscape, we collected reference-plots using a multi-scan set-up within equidistant 1 ha areas. Each reference plot was located within the footprint of the LR-TLS scans (Fig. 2). We placed six referenceplots in 100 m intervals up to a distance of 600 m from the vantage

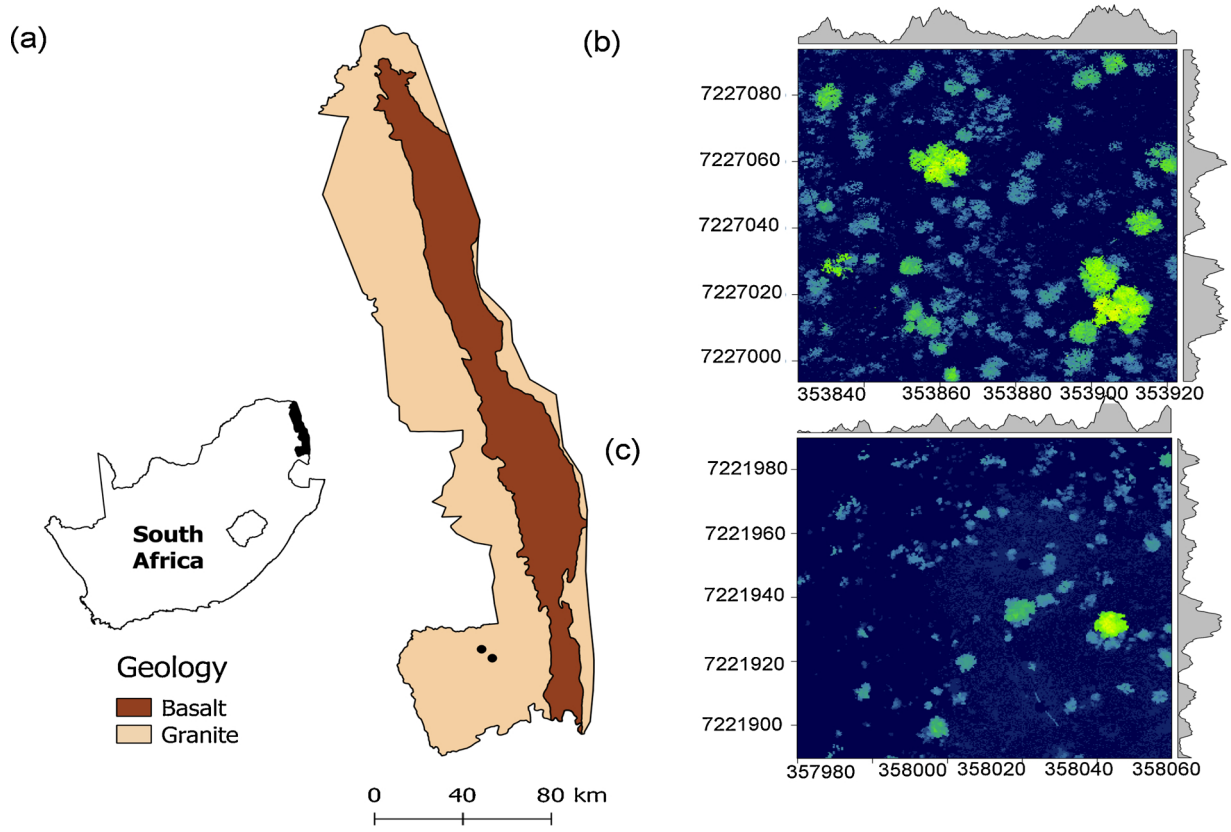

Fig. 1. (a) Location of the two sampling landscapes (shown with black circles) in Kruger National Park, South Africa. The rightmost panels show examples of 2D LiDAR data from the two sites, with the level-plots describing vegetation heterogeneity. Mathekinyani and Stevenson sites are shown in (b) and (c) respectively.

Table 1
Characteristics of two study landscapes located in Kruger National Park, South Africa. Canopy cover and slope are calculated from the multi-scan TLS data.

Site	Plot	Canopy cover (%)	Elevation (m)	Understorey	Slope (°)
KNP	Mathekinyani	52.21	12	Little	1.95
KNP	Stevenson	37.7	25	Little	3.13

Table 2
Specifications for the RIEGL VZ-2000 scanner utilized for the 3D long-range data acquisition in Kruger National Park, 2016.

Beam divergence	0.35 mrad
Pulse repetition rate	50 kHz
Angular sampling	0.02°
Maximum range	1500 m
Acquisition time	35 min

point. The reference-plots were scanned from the four cardinal directions at 550 kHz, with an angular resolution of 0.02°. The multi-scan approach captured the full 3D structure of the plots, providing a level of structural detail that cannot be achieved through manual field-measurement. As such, we treated these plots as ground-truth data against which to assess the LR-TLS (Fig. 3).

2.3. Point cloud processing

LR-TLS and reference-plot scans for each respective landscape were co-registered using the RiSCAN PRO package (RIEGL GmbH), to eliminate the rotation errors between different scans. A coarse registration between the scans was achieved by using large woody trees (branch tips and nodes) as the tie points. Fine tuning of translation and rotation errors within the scans was done by using multi-station adjustment (MSA) approach. MSA uses iterative closest point (ICP) algorithm to adjust the orientation and position of each 3D dataset, and calculates the best overall fit. The best fit transformation and rotation matrix are applied to each raw point cloud to associate them to a common co-ordinate system. The standard deviation for the distances between merged point clouds ranged from 0.01 to 0.02 m. The point clouds were post-processed to remove noise occurring due to partial or false returns from the sky or dust by using the range and deviation default filters in RiSCAN PRO.

The co-registered LiDAR data points from reference-plots and LR-TLS scans were then ground classified, and height normalized. Canopy height models (CHM) from normalized point clouds were generated by selecting the highest 'z' coordinate 3D point among all LiDAR returns within a '1 × 1 m' grid cell, thus converting the 3D data to raster for further analysis. The resulting canopy height grids were classified in SAGA GIS (www.saga-gis.org). LiDAR data between 0.0 and 0.5 m was classified as ground points, while all points above 0.5 m were categorized as vegetation. These classified grids were aggregated to percentage canopy cover at '30 × 30 m' for every reference and LR-TLS plots. The number of '1 × 1′m pixels in every '30 × 30 m' grid with height greater than 0.5 m were then divided by the total number of '1 × 1′ pixels in that grid, yielding the percentage of canopy cover present in each grid cell. For the comparison between LR-TLS and the reference-plots, difference values were derived by subtracting the value of each pixel of the LR-TLS raster from the corresponding pixel of the reference-plot raster.

Normalized point clouds were used to produce the LiDAR return counts from 0 m at every 0.5 m interval of the LiDAR data in LAStools (rapidlasso GmbH, 2014; Isenburg, 2014). These LiDAR counts were converted to percentage of frequency, and plotted against canopy

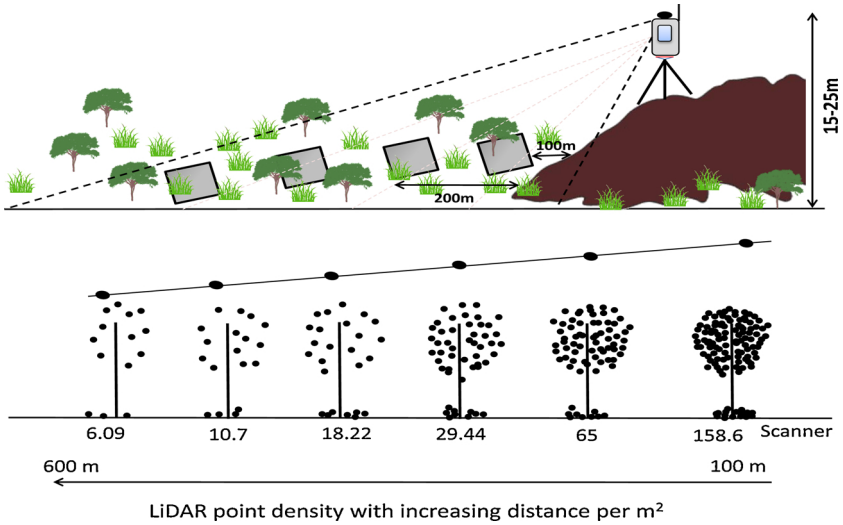

Fig. 2. Conceptual representation of the long-range scanning set-up adopted in this study. The black outlined grey squares indicate the multi-scan reference plots positioned 100 m apart from each other, and overlaid in the long-range scan footprint up to 600 m, with an associated decreases in point density.

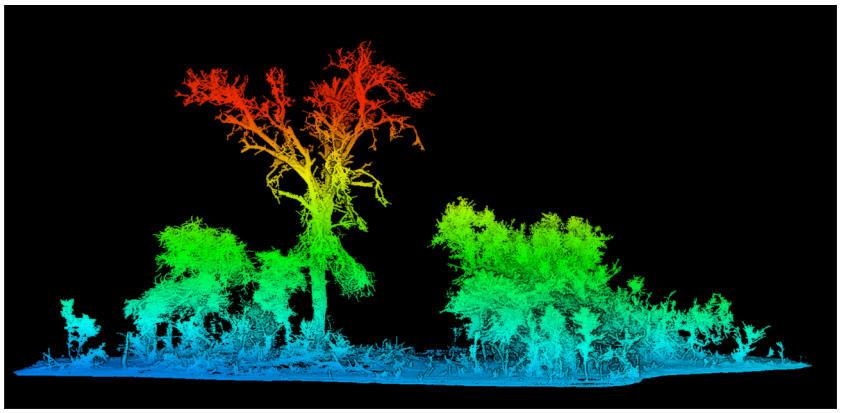

Fig. 3. Reference-plot example, derived from multi-scan TLS and shown in oblique view with color scale representing height above ground level. TLS instruments capture vegetation 3D structural detail in a holistic manner that cannot be recorded manually in the field. (For interpretation of the references to color in this figure legend, the reader is referred to the web version of this article.)

height to visualize the vertical vegetation profiles of the two sites.

2.4. TLS derived indicators for validation at individual tree scales

3D data collected from LR-TLS and reference-plots were used to estimate structural parameters for individual trees, such as the plant height (m) and ground projected area of the canopy (m^2). The individual trees and shrubs were extracted from the normalized LR-TLS and reference-plot scans, using Quick Terrain Modeler (www.appliedimagery.com). In each segmented tree and shrub, LiDAR measured plant height was determined as the vertical distance between the highest point and stem base at the ground. The segmented trees and shrubs were converted to raster form by generating the individual canopy height models (described in Section 2.3). Gaussian filtering with varying parameters were implemented on the individual trees and shrubs to smooth the canopy surface. A standard deviation of 1 and search radius ranging from 2 to 5 m was used in the Gaussian filter. The next step was applying the watershed segmentation, which assumes the presence of dark pixels in between tree crowns, where dark pixels represent ground surface while bright pixels represent tree canopies. To reduce the high degree of over-segmentation within a tree crown, threshold based region merging was implemented to amalgamate the segments. These segments were later converted to polygons and area geometry was calculated to extract canopy area. An individual watershed segmentation approach over plot-scale segmentation was implemented to overcome the high degree of segmentation within individual trees due to presence of multiple stem allometry.

2.5. Statistical analyses

To evaluate the effect of increasing distance on LR-TLS performance, we distributed a 30 × 30 m grid within overlapping footprints of the LR-TLS scans and the reference-plots, and extracted the height and canopy cover metrics. Statistically significant differences among canopy metrics from LR-TLS and reference plots were determined with a paired-sample *t*-test ($p < 0.05$). A linear regression between reference and long-range LiDAR woody cover and height at plot and individual scale was calculated and model performance was assessed with coefficient of determination (R^2). To account for the error propagation in the two sites, root mean square error (RMSE) and bias between LR-TLS and reference-plots was calculated.

Vertical height distribution profiles from the LR-TLS and reference-plots at increasing distance from the scanner were compared with respect to distribution patterns. To test whether increasing distance from the scanner had a significant effect on the vertical vegetation profiles, a two-tailed Mann Whitney *U* test was performed with a confidence interval of 0.05. The statistical significance was evaluated at 3 height classes – (i) 0–2.5 m (understorey and shrub), (ii) 2.5–5.5 m (midstorey) and (iii) 5–8 m (overstorey).

3. Results

3.1. Vegetation height-class characterization with LR-TLS

Comparison of the proportional distribution of LiDAR returns by

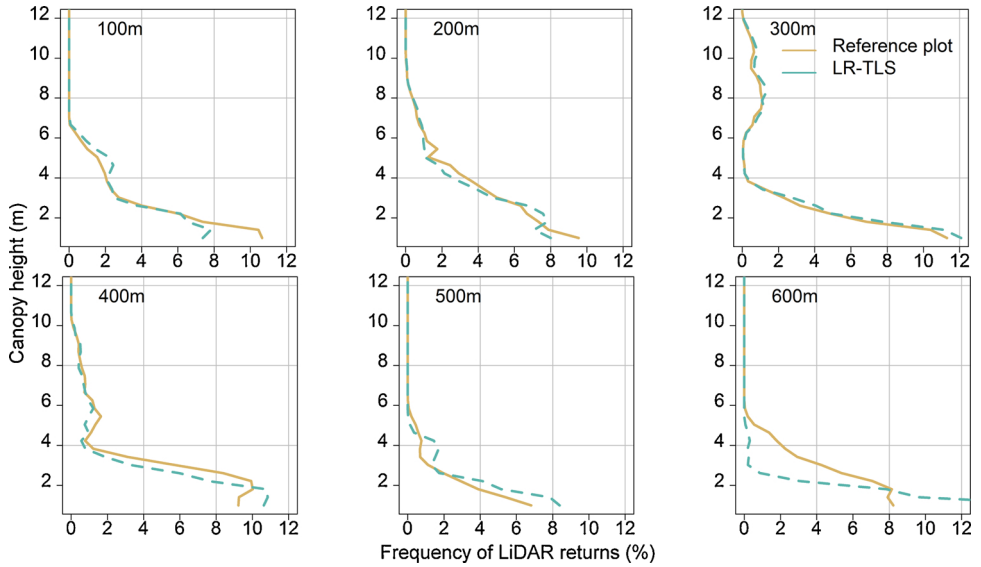

Fig. 4. Comparison of vertical height distribution derived from LR-TLS and reference-plots in vertical intervals of 0.5 m at increasing distances in the Mathekinyani landscape.

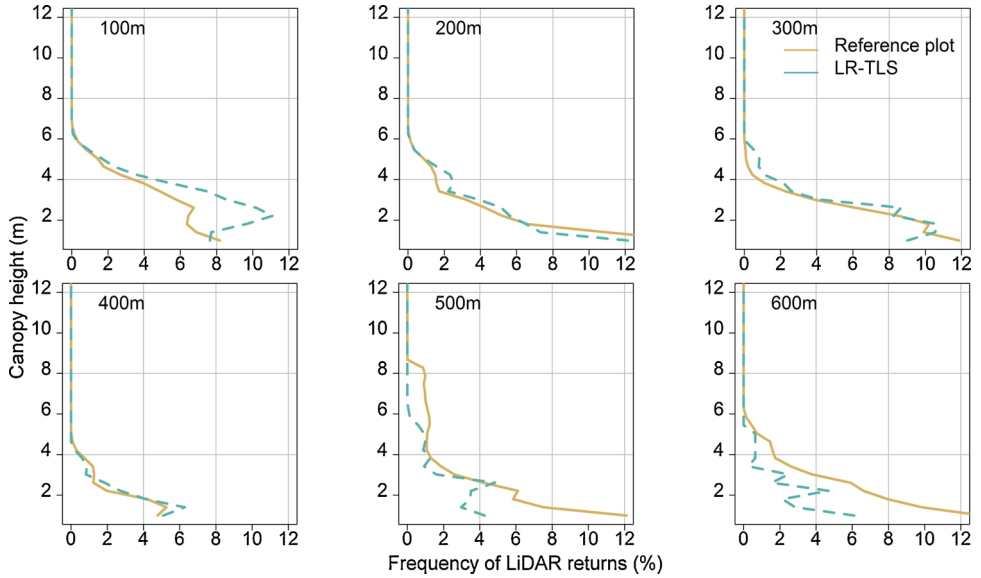

Fig. 5. Comparison of vertical height distribution derived from LR-TLS and reference plots in vertical intervals of 0.5 m with increasing distances in the Stevenson-Hamilton landscape.

height class showed that LR-TLS scans were capable of closely replicating the structure of the vertical vegetation profile of the savanna landscapes, despite their lower point density (Figs. 4 and 5). A general trend of increasing divergence between LR-TLS and reference-plot data was observed with increasing distance of laser ranging.

With a mean woody canopy cover of 52.21% within the 1 ha reference plots at the Mathekinyani site, the overall distribution of LiDAR returns at a distance of 100 m from the LR-TLS was analogous to the reference ($t = -1.84$, $df = 14$, $p = 0.08$) (Fig. 4). In general, up to a distance of 400 m, the LR-TLS derived vertical profiles represent a symmetric distribution with those of the reference-plots ($p > 0.05$, for the 3 height classes). At 500 m distance, significant differences in point distribution arose in the shortest height class ($p = 0.04$, $t = -2.92$, $df = 4$), while the relative distribution of points for the two taller classes was similar between LR-TLS and reference-plots ($t = 1.8331$, $df = 4$, $p = 0.14$).

Differences in vertical vegetation profiles in the Stevenson–Hamilton landscape were more variable across the range of distances explored. The shape of the vertical profiles was very similar up to 400 m distance ($p > 0.05$) (Fig. 5). However, some individual plots showed large discrepancy between the LR-TLS and reference profiles. For example, at 100 m distance there was a relatively greater proportion of returns from the mid-storey vegetation in the LR-TLS profiles than the reference-plot profiles, and deviated across the height range at distances of 500 and 600 m (Fig. 5).

3.2. Canopy height and cover differences

The overall distribution of canopy heights within the three defined height classes measured with LR-TLS correlated well with the reference-plot metrics, performing better at Mathekinyani ($R^2 = 0.80$) than at Stevenson-Hamilton ($R^2 = 0.54$) (Table 3) and (Fig. 6).

The performance of LR-TLS in the estimation of mean canopy height was similar among the two landscapes, and tended to slightly overestimate canopy height. Mean canopy height differences between the LR-TLS reference-plot values were not statistically different up to a

Table 3
The mean canopy height (m) values derived from reference plots (RP) and LR-TLS (LR). SD is the standard deviation.

Ranging distance (m)	Mathekinyani					Stevenson				
	RP_{mean}	RP_{SD}	LR_{mean}	LR_{SD}	p	RP_{mean}	RP_{SD}	LR_{mean}	LR_{SD}	p
100	1.49	0.26	1.31	0.25	0.33	2.92	0.58	2.61	0.45	0.14
200	1.50	2.19	1.78	0.51	0.38	1.95	0.37	1.33	0.41	0.02
300	2.25	1.10	2.51	0.62	0.54	3.08	1.02	2.10	0.64	0.08
400	1.53	0.51	1.97	0.54	0.11	0.98	0.37	0.70	0.51	0.47
500	1.35	0.58	1.45	1.05	0.12	3.17	2.12	1.55	0.74	0.05
600	2.73	0.41	1.43	0.55	0.79	1.49	0.47	1.20	0.59	0.26

distance range of 600 m in either landscape (Mathekinyani: $p = 0.79$, Stevenson: $p = 0.26$). Underestimation of the canopy height was greater (1.62 m difference) where undulating hillslopes and denser canopy was present, such as at the 500 m plot in Stevenson–Hamilton landscape, and negligible (0.10 m) on flatter more open sites.

Canopy cover estimates from LR-TLS demonstrated a high correlation with the reference-plot data, with slight overestimation in both landscapes (Table 4). Differences in canopy cover estimates increased exponentially with ranging distance, varying from 1% in the closer plots to a maximum of 15.43% in the distant plots (Fig. 6). Agreement between LR-TLS and reference-plots was best across plots on flatter terrain.

3.3. Individual tree metrics

For individual trees and shrubs, LR-TLS measured canopy heights were linearly correlated with the reference-plot data in both landscapes up to 400 m ranging distance ($R^2 = 0.99–0.87$, Fig. 7a and b). The detection of individual stems, especially shorter-statured shrubs, declined at distances greater than 500 m in both landscapes, resulting in an underestimation of height. The RMSE for the canopy height at the furthest measured plots (600 m) were 2.44 and 1.14 m respectively for Mathekinyani and Stevenson–Hamilton landscapes.

Canopy ground projected area for the individual trees can be determined with high confidence from the long-range scans up to 300 m of distance ($R^2 = 0.99–0.79$, Fig. 7c and d). As canopy ground projected

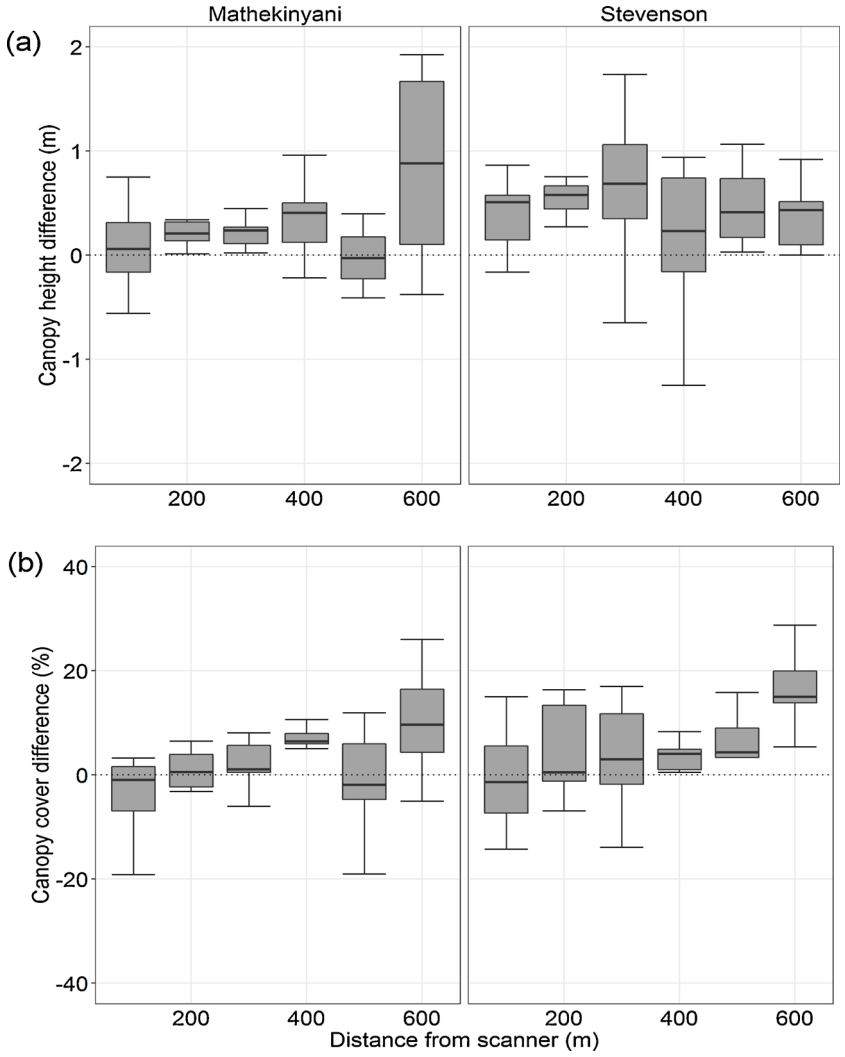

Fig. 6. Canopy height (a) and canopy cover (b) differences between LR-TLS and reference-plots with increasing ranging distance.

Table 4
Mean canopy cover (%) values derived from reference plots (RP) and LR-TLS (LR). SD is the standard deviation.

Ranging distance (m)	Mathekinyani					Stevenson				
	RP_{mean}	RP_{SD}	LR_{mean}	LR_{SD}	p	RP_{mean}	RP_{SD}	LR_{mean}	LR_{SD}	p
100	24.82	6.07	28.65	5.32	0.17	34.59	11.64	35.59	9.71	0.84
200	25.80	7.40	26.30	4.85	0.86	22.73	13.00	17.72	5.75	0.29
300	24.71	7.76	23.55	4.25	0.70	26.77	11.98	23.53	5.83	0.48
400	26.63	7.98	19.78	9.23	0.11	8.32	4.42	4.09	2.07	0.02
500	25.25	5.35	26.98	12.02	0.70	13.92	7.86	9.53	5.16	0.18
600	26.97	7.72	16.81	7.10	0.01	20.96	9.99	5.53	2.22	0.01

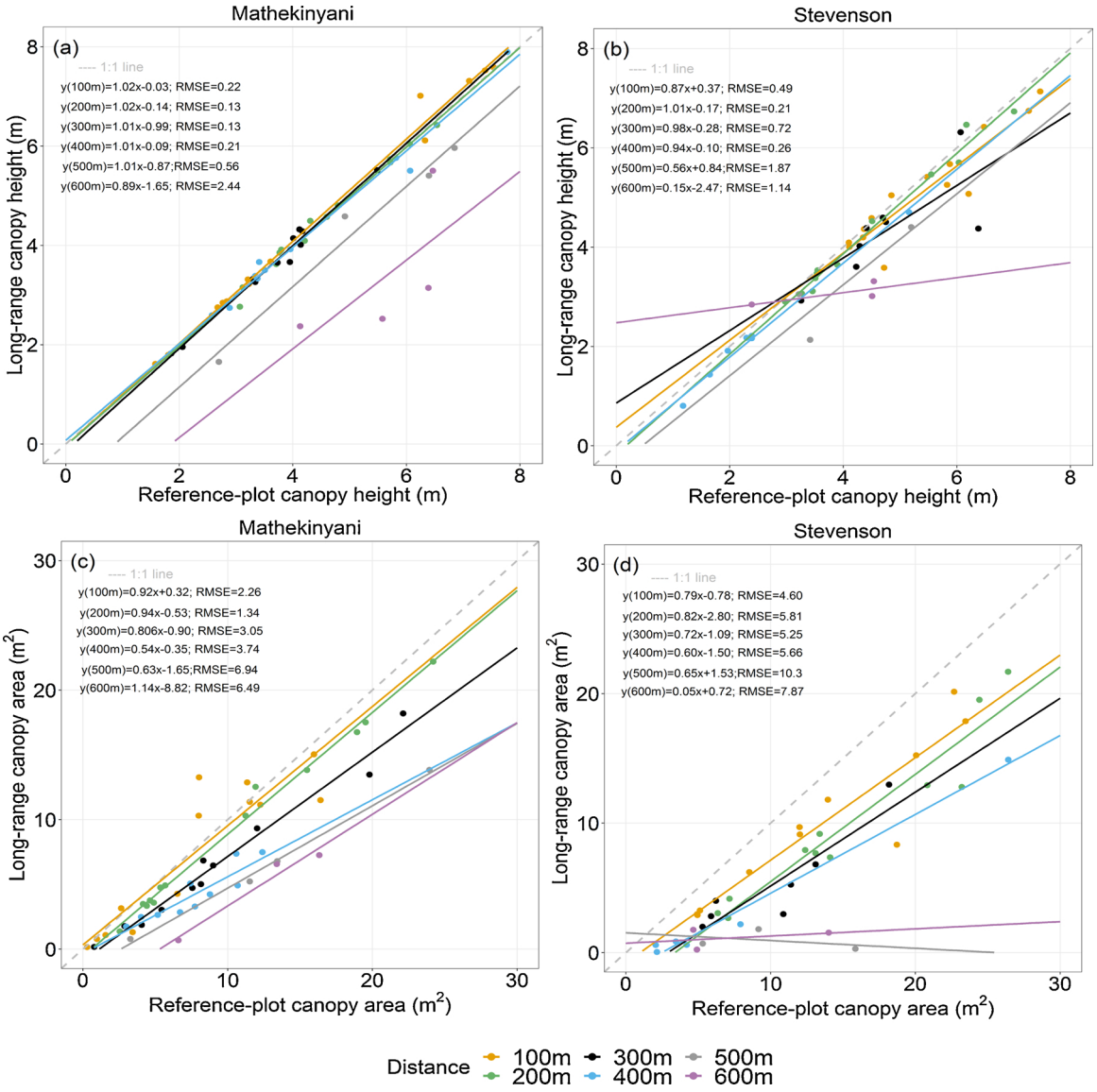

Fig. 7. (a) Deviation in canopy height, and (b) canopy ground projected area with increasing ranging distance in the two study landscapes. The color coding represents the linear interpolation model at different laser ranging distances. (For interpretation of the references to color in this figure legend, the reader is referred to the web version of this article.)

area is directly proportional to the point density, strong underestimation in the long-range scans is observed after a distance of 300 m (*RMSE* > 3.05). The linear regression model between reference and long-range scans differed at two sites, with the slopes of Stevenson site model diverging the most from the 1:1 reference line after a distance of 300 m (500 m: $R^2 = 0.16$, *RMSE* = 10.3; 600 m: $R^2 = 0.12$, *RMSE* = 7.87, Fig. 7c and d).

4. Discussion

Our results demonstrate the utility of long-range terrestrial laser scanning (LR-TLS) for quantifying savanna vegetation structural metrics at hillslope-scales. Despite the trade-offs of long range scanning (reduced point density and increased beam divergence at longer ranging distances), we found that vegetation structural parameters can be reliably extracted up to 500 m distance with LR-TLS in savanna

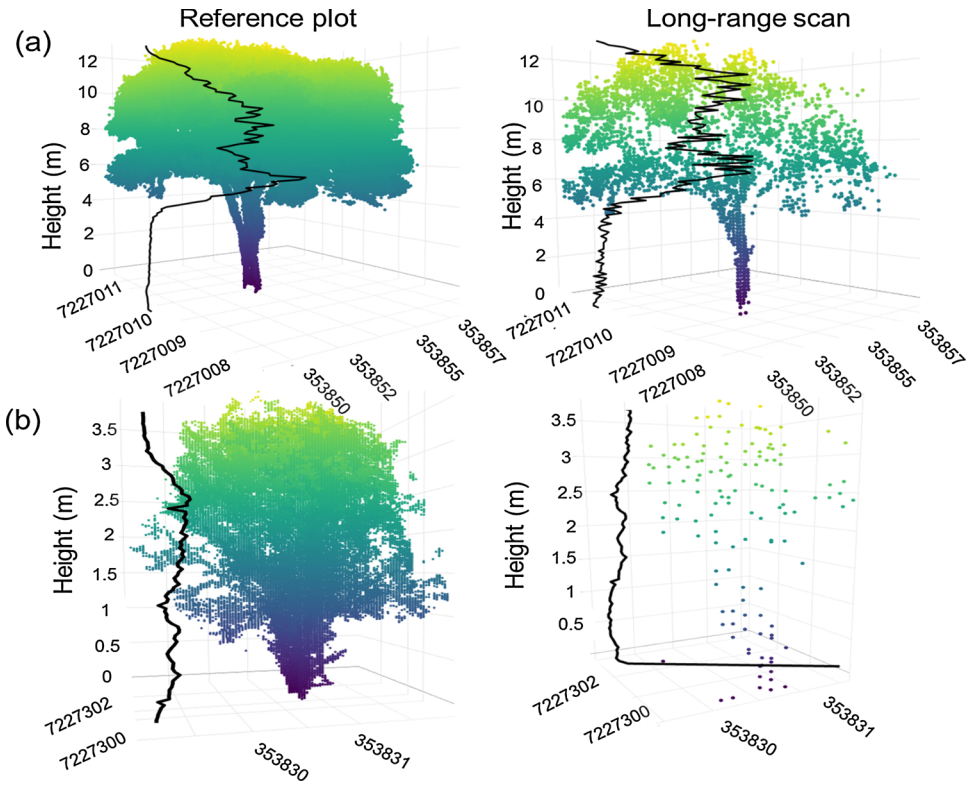

Fig. 8. An example of height normalized LiDAR returns of a single tree (a) and shrub (b) from reference-plots and LR-TLS at a ranging distance of 400 m.

landscapes, enabling structural sampling over broader areas that encompass the inherent heterogeneity.

4.1. The effect of increased ranging distance on the error propagation

LR-TLS and reference-plot vertical profiles were generally well matched, indicating that long-range scan observations can account for 3D vegetation structural patterns. The vegetation vertical profiles from LR-TLS mirrored the shape of the reference-plot profiles, with the relationships only degrading at ranging distances longer than 400–500 m. This effect arises from both the increased beam divergence, leading to reduced sensitivity to finer-scale vegetation elements, and a decrease in point density. We consider the decrease in point density to be a function of both the angular sampling resolution of the scanner, as well as site specific conditions which relate to increased occlusion from foreground vegetation and a loss of ground returns at lower incidence angles at longer ranging distances.

The reliable performance of height estimation from LR-TLS in our study landscapes was likely due to the presence of sparse canopies, and the clear lines of sight that characterize savanna landscapes. The accuracy of long-range scanning for vegetation metrics retrieval differed slightly among the two landscapes, reflecting differences in vegetation physiognomy and terrain morphology. Increased ranging distance from the scanner had less impact on canopy height retrieval in the Mathekinyani landscape, characterized by larger trees, than at the Stevenson–Hamilton landscape which was more shrub dominated. In addition to the distribution of taller trees, differences in canopy architecture due to leaf shape and branching angles, could have influenced these differences. For instance frequent crown openings in large tree dominated Mathekinyani landscape allowed a deeper penetration of the laser pulses, and thereby resulting in a low RMSE of 0.32 at 500 m distance. Srinivasan et al. (2015) also reported the underestimation of canopy height due to increasing canopy branching and distance from the scanner. Thus, when employing single scans for quantifying vegetation metrics, it is important to consider the laser pulse penetration through canopies to reduce the shadow effects and incomplete sampling of the vertical profiles. Also, some errors of the canopy height measurements at the Stevenson–Hamilton landscape occurred as a result of topographic effects, where occlusion from catenal hillslope crests caused a reduction in ground returns. At the longer distances of 600 m, this shadowing by topography can misrepresent the true tree height in the normalization phase of the processing chain. This potentially leads to canopy height bias because accurate representation of the terrain is crucial for calculating the canopy height models.

These factors discussed above are also relevant for the estimation of the canopy cover, however as cover is an area based measure further considerations also apply. The high deviation and RMSE of canopy cover estimates after 400 m can be attributed to the occlusion of lower strata vegetation, the step size, at which 'z' value is interpolated for every output pixel of the CHM, and the window size for subsequent analysis. Decreased sensitivity to smaller vegetation individuals and components with ranging distance leads to a cumulative decline in canopy cover estimates. Usually a step size close to the laser spot size is recommended for resolving small vegetation individuals (Khosravipour et al., 2014), however we found that small vegetation elements and understorey plants cannot be reliably identified by keeping the same step size with increasing distance from the LR-TLS. Laser spot size for Riegl VZ-2000 increases by 0.3 mm per 100 m of range (Riegl VZ-2000 datasheet), and as such the step size should therefore be adjusted at every 100 m range to account for the increasing beam diameter. The window size used for subsequent analyses also strongly influenced the accuracy of canopy cover estimates derived from LR-TLS. We found that the RMSE and linear regression model fits improved as window size increased from 0.09 to 1 ha. Though, Wilkes et al. (2017) describes 10×10 m sampling grid as an upper size limit for characterizing vegetation structure in homogeneous and closed canopy sites. However, in a heterogeneous savanna landscape, trees are non-uniform in size and widely spaced, providing enough laser pulse penetration through the sampled area. Also, large plot sizes result in fewer plot-edge effect, due to presence of tree crowns located outside the plot (Levick et al.,

2016).

For individual large trees, LR-TLS accurately depicted the structure at ranging distances up to 400 m. Even small branches were documented at these distances, and the branching structure was retained in the LR-TLS data (Fig. 8a). While LR-TLS could characterize the shrub height reliably, the internal canopy structure of shrubs in the farthest plots could not be differentiated (Fig. 8b).

Underestimation of individual tree height with increased ranging distance was most often due to the loss of the lower stem architecture and ground points. Denser scan patterns, i.e. multi-scan approaches, increases the ability to resolve the stem architecture, particularly towards the ground, and therefore increases the fidelity of canopy height and projected area estimates. Larger differences in individual tree canopy height and ground projected area at distances further than 300 m were particularly evident in the Stevenson-Hamilton landscape, where presence of undulating terrain and a slope of 3.1° led to the attenuation of laser pulses and more occlusion.

4.2. Reliable quantification of 3D vegetation structure at hillslope-scales

LR-TLS suitably captured vegetation structural measures such as height, height profile distribution, and canopy cover at both plot and individual tree scales at distances of up to 400 and 500 m in the two landscape we studied. Earlier studies demonstrate, that the utilization of TLS to estimate vegetation metrics is confined only to 0.01–1-ha spatial scale (Beland et al., 2019). In our study, if we consider 400 m as conservative range for reliable structural quantification, LR-TLS could theoretically be used to sample 50 ha of landscape in a single scan – taking less than 1 hour with the settings used in this study. Of course this is assuming a full 360° scan from a point elevated above the canopy, which is not feasible in many situations. Nonetheless, even if only 180° or 90° scanning is possible – this approach still enables the acquisition of 3D structural data over 10's ha – scales that are required to adequately represent the heterogeneity of savanna ecosystems. Even larger areas can potentially be reliably mapped with the proposed method, if the vegetation is not obscured by occlusion and if the survey position can be elevated higher above the canopy. Topographic occlusion in the sampled areas was lowest at the Mathekinyani landscape, while the 3D point cloud at Stevenson–Hamilton displayed greater occlusion. The amount of occlusion also varied with vegetation physiognomy and distribution, as well as the height of the sensor in relation to the landscape. A sparse canopy and a mean nearest difference of 2–3 m between individuals was sufficient to prevent the attenuation of laser pulses in the Mathekinyani landscape. Also, the wider beam diameter at increasing distance (beam diameter = 0.3 m at 1000 m) from the scanner reduced the penetration through the understorey. Ducey et al. (2013), suggested that a small beam diameter leads to a better penetration through low branches and understorey vegetation. Raising the scanner higher above the canopy layer is the best option for reducing the occlusion effect, but statistical methods can also be employed to adjust the effects of occlusion (Strahler et al., 2008; Lovell et al., 2011).

With a high angular resolution of 0.02°, 3D point clouds with a density of $> 5/m^2$, at distances up to 600 m was produced, allowing long-distance scans to capture a large proportion of the target canopies and tree individuals. Point density diluted exponentially as the distance to the scanner increased, resulting in a heterogeneous point density. Many studies have reported that heterogeneous point density from single scanning mode has no adverse effect on the retrieval of physical attributes such as canopy height and cover (Thies and Spiecker, 2004; Maas et al., 2008; Moskal and Zheng, 2011), but ours is the first to explore the consequences over such long distances. Uniform point density is often required for clustering and classification of 3D point clouds with semi-automatic approaches (Olofsson et al., 2014), but this could be achieved by sub-sampling the point clouds if needed.

4.3. Limitations and future direction for large scale monitoring of savanna vegetation

Our use of LR-TLS has provided an alternative method for characterizing savanna vegetation structure at hillslope scales. However, we acknowledge a few limitations of this approach, which should direct new research and method development in this direction. First, our results may not extrapolate well from open savanna to other vegetation communities. For example, at riparian sites occlusion by dense understorey layers will inhibit deep laser pulse penetration up to 400 m. Also, performance of the LR-TLS will differ among flat and undulating terrain, with more bias in canopy height measurements in landscapes with undulating morphology. In general, occlusion could be reduced by acquiring multiple LR-TLS scans from different positions. Second, our study explored the efficiency of LR-TLS over two landscapes in open savanna, and a larger sample size will be required to ascertain the generality of this method in different systems. Third, our use of LR-TLS is unique in that the scanner was positioned above the canopy to capture hillslope-scale 3D data. We had the advantage of the elevated vantage points, but at other sites alternatives such as elevating tripods or vehicle roof top mounts can be explored. Lastly, the individual plant scale analysis required a high degree of processing from extracting single trees from the point cloud data to calculating canopy area of individual trees. Although much progress has been made on automating these tasks in forested systems (Burt et al., 2018), these techniques need further development before they can be successfully applied to savanna tree structures which are more complex. This opens up the possibility of testing various automatic segmentation approaches for single tree extraction from LR-TLS, and subsequently realizing the potential of open access tools such as ForestR (Atkins et al., 2018) in defining the vegetation complexity.

In the next few years, vegetation structural information will be available from a number of satellite missions, including L- and S-band SAR (NISAR), P-band SAR (BIOMASS), spaceborne ISS-mounted LiDAR (GEDI) and ICESat-2. These products will facilitate mapping at regional and global scales, and will complement the availability of open-access and high spatio-temporal resolution imagery from the Sentinel platforms – providing very valuable opportunity for fine characterization of savanna vegetation at landscape to regional scales. While the data collection capabilities can always be enhanced, the real challenges for applying these sensors to large area monitoring are calibration and validation. Field-based plot inventory data are not suitable in isolation, and while airborne LiDAR currently plays a key role and will continue to do so, we also need to explore new ways for reducing uncertainty in biomass allometries and upscaling models. For open tree-grass systems and shrublands, the LR-TLS approach presented in this paper can provide the continuum of ground reference data that can also encompass stand variation. This has the potential to improve the spatial extrapolation of vegetation structure from remote sensing proxies, which is a key to reducing uncertainties in the global carbon budget. Furthermore, the fixed scanning position of LR-TLS will enable repeat measurements of higher precision than what is possible from aircraft or UAV platforms, opening the door for examining fine-scale dynamics in vegetation canopies over hillslope scales. This is particularly relevant in savanna ecosystems, where future research should explore the potential of repeat LR-TLS to analyze structural changes over time for understanding the loss of big trees and patterns of woody encroachment (Levick and Asner, 2013; Lindenmayer et al., 2012).

4.4. Conclusions

Our exploration of long-range terrestrial scanning (LR-TLS) shows great promise for the reliable extraction of inventory parameters of savanna woody vegetation including canopy height, vertical profile distribution, and canopy cover at hillslope scales. Plot and individual tree level metrics can be accurately retrieved from ranging distances of

400 m, meaning that 10–50 ha can be sampled in under one hour depending on the landscape. The use of LR-TLS for vegetation mapping in savanna will help to overcome a key limitation of TLS in terms of limited spatial extent, enabling measurement and monitoring at hillslope-scales. LR-TLS will provide a useful tool to complement field and airborne surveys in the direct calibration and validation of satellite derived biophysical attributes.

Authors' contribution

Jenia Singh: data acquisition, methodology, software, data processing, analysis, visualization, writing original draft. Shaun R. Levick: conceptualization, data acquisition, supervision, reviewing and editing. Marcus Guderle: data acquisition, processing, software and reviewing. Christiane Schmullius: supervision.

Conflict of interest

None declared.

Acknowledgements

We thank South African National Parks for granting permission to conduct this study in Kruger National Park. Izak Smit, Navashni Govender, and Tercia Strydom are acknowledged for their help and support for this research. We thank all the game guards for their help in the field. J.S. is funded by the Max-Planck-Gesellschaft (MPG)through its International Max Planck Research School for Global Biogeochemical Cycles (IMPRS-gBGC). We also thank Susan Trumbore for her helpful comments on the manuscript.

References

Archibald, S., Lehmann, C.E., Gómez-Dans, J.L., Bradstock, R.A., 2013. Defining pyromes and global syndromes of fire regimes. Proc. Natl. Acad. Sci. U.S.A. 201211466.
Asner, G.P., Knapp, D.E., Kennedy-Bowdoin, T., Jones, M.O., Martin, R.E., Boardman, J.W., Field, C.B., 2007. Carnegie airborne observatory: in-flight fusion of hyperspectral imaging and waveform light detection and ranging for three-dimensional studies of ecosystems. J. Appl. Rem. Sens. 1, 13536.
Asner, G.P., Levick, S.R., Kennedy-Bowdoin, T., Knapp, D.E., Emerson, R., Jacobson, J., Colgan, M.S., Martin, R.E., 2009. Large-scale impacts of herbivores on the structural diversity of African savannas. Proc. Natl. Acad. Sci. U.S.A. 106, 4947–4952.
Astrup, R., Ducey, M.J., Granhus, A., Ritter, T., von Lüpke, N., 2014. Approaches for estimating stand-level volume using terrestrial laser scanning in a single-scan mode. Can. J. Forest Res. 44, 666–676.
Atkins, J.W., Bohrer, G., Fahey, R.T., Hardiman, B.S., Morin, T.H., Stovall, A.E., Zimmerman, N., Gough, C.M., 2018. Quantifying vegetation and canopy structural complexity from terrestrial LiDAR data using the forestr R package. Methods Ecol. Evol. 9, 2057–2066.
Beland, M., Parker, G., Sparrow, B., Harding, D., Chasmer, L., Phinn, S., Antonarakis, A., Strahler, A., 2019. On promoting the use of LiDAR systems in forest ecosystem research. Forest Ecol. Manag. 450, 117484.
Boggs, G., 2010. Assessment of spot 5 and quickbird remotely sensed imagery for mapping tree cover in savannas. Int. J. Appl. Earth Observ. Geoinform. 12, 217–224.
Buitenwerf, R., Bond, W., Stevens, N., Trollope, W., 2012. Increased tree densities in south African savannas: 50 years of data suggests CO2 as a driver. Glob. Change Biol. 18, 675–684.
Burt, A., Disney, M., Calders, K., 2018. Extracting individual trees from LiDAR point clouds using treeseg. Methods Ecol. Evol.
Calders, K., Armston, J., Newnham, G., Herold, M., Goodwin, N., 2014. Implications of sensor configuration and topography on vertical plant profiles derived from terrestrial LiDAR. Agric. Forest Meteorol. 194, 104–117.
Calders, K., Newnham, G., Burt, A., Murphy, S., Raumonen, P., Herold, M., Culvenor, D., Avitabile, V., Disney, M., Armston, J., et al., 2015. Nondestructive estimates of above-ground biomass using terrestrial laser scanning. Methods Ecol. Evol. 6, 198–208.
Calders, K., Origo, N., Burt, A., Disney, M., Nightingale, J., Raumonen, P., Åkerblom, M., Malhi, Y., Lewis, P., 2018. Realistic forest stand reconstruction from terrestrial LiDAR for radiative transfer modelling. Rem. Sens. 10, 933.
Dassot, M., Colin, A., Santenoise, P., Fournier, M., Constant, T., 2012. Terrestrial laser scanning for measuring the solid wood volume, including branches, of adult standing trees in the forest environment. Comput. Electron. Agric. 89, 86–93.
Disney, M.I., Boni Vicari, M., Burt, A., Calders, K., Lewis, S.L., Raumonen, P., Wilkes, P., 2018. Weighing trees with lasers: advances, challenges and opportunities. Interface Focus 8, 20170048.
Dittmann, S., Thiessen, E., Hartung, E., 2017. Applicability of different non-invasive methods for tree mass estimation: a review. Forest Ecol. Manag. 398, 208–215.
Dubayah, R.O., Drake, J.B., 2000. LiDAR remote sensing for forestry. J. Forestry 98, 44–46.
Ducey, M.J., Astrup, R., Seifert, S., Pretzsch, H., Larson, B.C., Coates, K.D., 2013. Comparison of forest attributes derived from two terrestrial LiDAR systems. Photogram. Eng. Rem. Sens. 79, 245–257.
Ehbrecht, M., Schall, P., Ammer, C., Seidel, D., 2017. Quantifying stand structural complexity and its relationship with forest management, tree species diversity and microclimate. Agric. Forest Meteorol. 242, 1–9.
Frazer, G., Magnussen, S., Wulder, M., Niemann, K., 2011. Simulated impact of sample plot size and co-registration error on the accuracy and uncertainty of LiDAR-derived estimates of forest stand biomass. Rem. Sens. Environ. 115, 636–649.
Gertenbach, W.D., 1983. Landscapes of the Kruger National Park. Koedoe 26, 9–121.
Gonzalez de Tanago, J., Lau, A., Bartholomeus, H., Herold, M., Avitabile, V., Raumonen, P., Martius, C., Goodman, R.C., Disney, M., Manuri, S., et al., 2018. Estimation of above-ground biomass of large tropical trees with terrestrial LiDAR. Methods Ecol. Evol. 9, 223–234.
Grace, J., José, J.S., Meir, P., Miranda, H.S., Montes, R.A., 2006. Productivity and carbon fluxes of tropical savannas. J. Biogeogr. 33, 387–400.
Hardiman, B., LaRue, E., Atkins, J., Fahey, R., Wagner, F., Gough, C., 2018. Spatial variation in canopy structure across forest landscapes. Forests 9, 474.
Hilker, T., van Leeuwen, M., Coops, N.C., Wulder, M.A., Newnham, G.J., Jupp, D.L., Culvenor, D.S., 2010. Comparing canopy metrics derived from terrestrial and airborne laser scanning in a Douglas-fir dominated forest stand. Trees 24, 819–832.
Hopkinson, C., Chasmer, L., Young-Pow, C., Treitz, P., 2004. Assessing forest metrics with a ground-based scanning LiDAR. Can. J. Forest Res. 34, 573–583.
Isenburg, M., 2014. Lastools-Efficient LiDAR Processing Software (Version 140929). rapidlasso GmbH, Gilching.
Khosravipour, A., Skidmore, A.K., Isenburg, M., Wang, T., Hussin, Y.A., 2014. Generating pit-free canopy height models from airborne LiDAR. Photogram. Eng. Rem. Sens. 80, 863–872.
Lefsky, M.A., Cohen, W.B., Parker, G.G., Harding, D.J., 2002. LiDAR remote sensing for ecosystem studies: LiDAR, an emerging remote sensing technology that directly measures the three-dimensional distribution of plant canopies, can accurately estimate vegetation structural attributes and should be of particular interest to forest, landscape, and global ecologists. AIBS Bull. 52, 19–30.
Levick, S., Rogers, K., 2008. Structural biodiversity monitoring in savanna ecosystems: integrating LiDAR and high resolution imagery through object-based image analysis. Object-Based Image Analysis 477–491.
Levick, S.R., Asner, G.P., 2013. The rate and spatial pattern of treefall in a savanna landscape. Biol. Conserv. 157, 121–127.
Levick, S.R., Hessenmöller, D., Schulze, E.D., 2016. Scaling wood volume estimates from inventory plots to landscapes with airborne LiDAR in temperate deciduous forest. Carbon Balance Manag. 11, 7.
Levick, S.R., Rogers, K.H., 2011. Context-dependent vegetation dynamics in an African savanna. Landsc. Ecol. 26, 515–528.
Liang, X., Kankare, V., Hyyppä, J., Wang, Y., Kukko, A., Haggrén, H., Yu, X., Kaartinen, H., Jaakkola, A., Guan, F., et al., 2016. Terrestrial laser scanning in forest inventories. ISPRS J. Photogram. Rem. Sens. 115, 63–77.
Lindenmayer, D.B., Laurance, W.F., Franklin, J.F., 2012. Global decline in large old trees. Science 338, 1305–1306.
Lovell, J., Jupp, D., Newnham, G., Culvenor, D., 2011. Measuring tree stem diameters using intensity profiles from ground-based scanning LiDAR from a fixed viewpoint. ISPRS J. Photogram. Rem. Sens. 66, 46–55.
Lucas, R.M., Armston, J., 2007. Alos palsar for characterizing wooded savannas in northern Australia. IEEE International Geoscience and Remote Sensing Symposium, IGARSS 2007 3610–3613.
Maas, H.G., Bienert, A., Scheller, S., Keane, E., 2008. Automatic forest inventory parameter determination from terrestrial laser scanner data. Int. J. Rem. Sens. 29, 1579–1593.
MacFadyen, S., Zambatis, N., Van Teeffelen, A.J., Hui, C., 2018. Long-term rainfall regression surfaces for the Kruger National Park, South Africa: a spatio-temporal review of patterns from 1981 to 2015. Int. J. Climatol. 38, 2506–2519.
Mathieu, R., Naidoo, L., Cho, M.A., Leblon, B., Main, R., Wessels, K., Asner, G.P., Buckley, J., Van Aardt, J., Erasmus, B.F., et al., 2013. Toward structural assessment of semi-arid African savannahs and woodlands: The potential of multitemporal polarimetric radarsat-2 fine beam images. Rem. Sens. Environ. 138, 215–231.
Meyer, K.M., Wiegand, K., Ward, D., Moustakas, A., 2007. The rhythm of savanna patch dynamics. J. Ecol. 95, 1306–1315.
Moskal, L.M., Zheng, G., 2011. Retrieving forest inventory variables with terrestrial laser scanning (TLS) in urban heterogeneous forest. Rem. Sens. 4, 1–20.
Muir, J., Phinn, S., Eyre, T., Scarth, P., 2018. Measuring plot scale woodland structure using terrestrial laser scanning. Rem. Sens. Ecol. Conserv.
Newnham, G.J., Armston, J.D., Calders, K., Disney, M.I., Lovell, J.L., Schaaf, C.B., Strahler, A.H., Danson, F.M., 2015. Terrestrial laser scanning for plot-scale forest measurement. Curr. Forestry Rep. 1, 239–251.
Olofsson, K., Holmgren, J., Olsson, H., 2014. Tree stem and height measurements using terrestrial laser scanning and the ransac algorithm. Rem. Sens. 6, 4323–4344.
Olofsson, K., Olsson, H., 2018. Estimating tree stem density and diameter distribution in single-scan terrestrial laser measurements of field plots: a simulation study. Scand. J. Forest Res. 33, 365–377.
Paynter, I., Genest, D., Saenz, E., Peri, F., Boucher, P., Li, Z., Strahler, A., Schaaf, C., 2018. Classifying ecosystems with metaproperties from terrestrial laser scanner data. Methods Ecol. Evol. 9, 210–222.
Saarinen, N., Kankare, V., Vastaranta, M., Luoma, V., Pyörälä, J., Tanhuanpää, T., Liang, X., Kaartinen, H., Kukko, A., Jaakkola, A., et al., 2017. Feasibility of terrestrial laser

scanning for collecting stem volume information from single trees. ISPRS J. Photogram. Rem. Sens. 123, 140–158.
Sankaran, M., Ratnam, J., Hanan, N., 2008. Woody cover in African savannas: the role of resources, fire and herbivory. Glob. Ecol. Biogeogr. 17, 236–245.
Scholes, R., Archer, S., 1997. Tree-grass interactions in savannas. Annu. Rev. Ecol. Systemat. 28, 517–544.
Seidel, D., Ammer, C., 2014. Efficient measurements of basal area in short rotation forests based on terrestrial laser scanning under special consideration of shadowing. iForest-Biogeosci. Forest. 7, 227.
Singh, J., Levick, S., Guderle, M., Schmullius, C., Trumbore, S., 2018. Vegetation physiognomy and biomass in semi-arid savanna. Ecosphere 9.
Srinivasan, S., Popescu, S.C., Eriksson, M., Sheridan, R.D., Ku, N.W., 2015. Terrestrial laser scanning as an effective tool to retrieve tree level height, crown width, and stem diameter. Rem. Sens. 7, 1877–1896.
Staben, G., Lucieer, A., Scarth, P., 2018. Modelling LiDAR derived tree canopy height from landsat TM, ETM+ and OLI satellite imagery – a machine learning approach. Int. J. Appl. Earth Observ. Geoinform. 73, 666–681.
Stevens, N., Lehmann, C.E., Murphy, B.P., Durigan, G., 2017. Savanna woody encroachment is widespread across three continents. Glob. Change Biol. 23, 235–244.
Stovall, A.E., Anderson-Teixeira, K.J., Shugart, H.H., 2018. Assessing terrestrial laser scanning for developing non-destructive biomass allometry. Forest Ecol. Manag. 427, 217–229.
Strahler, A.H., Jupp, D.L., Woodcock, C.E., Schaaf, C.B., Yao, T., Zhao, F., Yang, X., Lovell, J., Culvenor, D., Newnham, G., et al., 2008. Retrieval of forest structural parameters using a ground-based LiDAR instrument (echidna®). Can. J. Rem. Sens. 34, S426–S440.
Thies, M., Spiecker, H., 2004. Evaluation and future prospects of terrestrial laser scanning for standardized forest inventories. Forest 2, 1.
Urbazaev, M., Thiel, C., Mathieu, R., Naidoo, L., Levick, S.R., Smit, I.P., Asner, G.P., Schmullius, C., 2015. Assessment of the mapping of fractional woody cover in southern African savannas using multi-temporal and polarimetric alos palsar l-band images. Rem. Sens. Environ. 166, 138–153.
Vaughn, N.R., Asner, G.P., Smit, I.P., Riddel, E.S., 2015. Multiple scales of control on the structure and spatial distribution of woody vegetation in African savanna watersheds. PLOS ONE 10, e0145192.
Venter, F., 1986. Soil patterns associated with the major geological units of the Kruger National Park. Koedoe 29, 125–138.
Wigley, B.J., Bond, W.J., Hoffman, M.T., 2010. Thicket expansion in a south african savanna under divergent land use: local vs. global drivers? Glob. Change Biol. 16, 964–976.
Wilkes, P., Lau, A., Disney, M., Calders, K., Burt, A., de Tanago, J.G., Bartholomeus, H., Brede, B., Herold, M., 2017. Data acquisition considerations for terrestrial laser scanning of forest plots. Rem. Sens. Environ. 196, 140–153.
Williams, R.J., Hutley, L.B., Cook, G.D., Russell-Smith, J., Edwards, A., Chen, X., 2004. Assessing the carbon sequestration potential of mesic savannas in the Northern Territory, Australia: approaches, uncertainties and potential impacts of fire. Funct. Plant Biol. 31, 415–422.